Biogeosciences

Seasonal development of iron limitation in the sub-Antarctic zone

Thomas J. Ryan-Keogh[1,2], **Sandy J. Thomalla**[1,3], **Thato N. Mtshali**[1], **Natasha R. van Horsten**[1,4], **and Hazel J. Little**[2]

[1]Southern Ocean Carbon and Climate Observatory, Natural Resources and Environment,
CSIR, Rosebank, Cape Town, 7700, South Africa
[2]Department of Oceanography, University of Cape Town, Rondebosch, Cape Town, 7701, South Africa
[3]Marine Research Institute, University of Cape Town, Rondebosch, Cape Town, 7701, South Africa
[4]Department of Earth Sciences, Stellenbosch University, Stellenbosch, 7600, South Africa

Correspondence: Thomas J. Ryan-Keogh (tryankeogh@csir.co.za)

Abstract. The seasonal and sub-seasonal dynamics of iron availability within the sub-Antarctic zone (SAZ; ~ 40–$45°$ S) play an important role in the distribution, biomass and productivity of the phytoplankton community. The variability in iron availability is due to an interplay between winter entrainment, diapycnal diffusion, storm-driven entrainment, atmospheric deposition, iron scavenging and iron recycling processes. Biological observations utilizing grow-out iron addition incubation experiments were performed at different stages of the seasonal cycle within the SAZ to determine whether iron availability at the time of sampling was sufficient to meet biological demands at different times of the growing season. Here we demonstrate that at the beginning of the growing season, there is sufficient iron to meet the demands of the phytoplankton community, but that as the growing season develops the mean iron concentrations in the mixed layer decrease and are insufficient to meet biological demand. Phytoplankton increase their photosynthetic efficiency and net growth rates following iron addition from midsummer to late summer, with no differences determined during early summer, suggestive of seasonal iron depletion and an insufficient resupply of iron to meet biological demand. The result of this is residual macronutrients at the end of the growing season and the prevalence of the high-nutrient low-chlorophyll (HNLC) condition. We conclude that despite the prolonged growing season characteristic of the SAZ, which can extend into late summer/early autumn, results nonetheless suggest that iron supply mechanisms are insufficient to maintain potential maximal growth and productivity throughout the season.

1 Introduction

The Southern Ocean is an important region for atmospheric CO_2 drawdown, with 30–40 % of global anthropogenic carbon uptake (Khatiwala et al., 2009; Mikaloff Fletcher et al., 2006; Schlitzer, 2002), which is driven by local phytoplankton community production and the biological carbon pump (BCP). The BCP is, however, sensitive to environmental influences that are associated with climate change, which include an intensification of the westerly winds (Le Quéré et al., 2009), and altered upwelling and mixed-layer stratification (Bopp et al., 2005; Boyd, 2002). Together, these changes will impact the light and nutrient supply to the phytoplankton community, which could in turn alter the efficiency and extent of the BCP in the future.

The high productivity characteristic of this region is driven in part by the high macronutrient availability, while phytoplankton growth and productivity are ultimately constrained by the availability of light and iron (de Baar et al., 1990; Martin et al., 1990). The result of this limitation is the prevalence of macronutrients in the surface waters at the end of the growing season, resulting in the paradoxical high-nutrient low-chlorophyll (HNLC) conditions characteristic of the region. Further controls on the seasonal evolution and extent of the phytoplankton bloom include potential silicate limitation (Boyd et al., 2010; Hutchins et al., 2001), top–down controls by meso- and micro-zooplankton grazing (Dubischar and Bathmann, 1997; Moore et al., 2013; Pakhomov and Froneman, 2004; Smetacek et al., 2004), and seasonal–sub-seasonal changes in the critical and mixed-layer depths (Fauchereau et al., 2011; Nelson and Smith, 1991).

Iron is a key component of photosynthesis due to the high requirements in the formation and function of key photosynthetic proteins, including photosystem I and photosystem II (Raven, 1990; Raven et al., 1999; Shi et al., 2007; Strzepek and Harrison, 2004). In addition, iron requirements by phytoplankton are closely linked to light availability, displaying an inverse relationship. Under low-light conditions phytoplankton can maximize photosynthesis in different ways by either increasing the size or number of their photosynthetic units, the latter resulting in an increase in iron requirements under low light (Maldonado et al., 1999; Raven, 1990; Strzepek et al., 2011, 2012; Sunda and Huntsman, 1997). This close coupling of light and iron, which increases the cellular demand for iron under low-light conditions, can diminish light-dependent photosynthesis when iron concentrations are too low to support growth (Hiscock et al., 2008; Moore et al., 2013; Ryan-Keogh et al., 2017b). Iron is also required in the function of both nitrate and nitrite reductase (de Baar et al., 2005), which function to facilitate the assimilation of nitrate and nitrite and their subsequent intracellular reduction to ammonium. In the Southern Ocean, and other HNLC areas, nitrate uptake rates are reported as becoming iron-limited for this reason (Cochlan, 2008; Lucas et al., 2007; Moore et al., 2013; Price et al., 1994). However, rather than iron limitation directly inhibiting nitrate and nitrite reductase activity, the cause of reduced uptake rates may be a bottleneck further downstream due to a lack of photosynthetically derived reductant (Milligan and Harrison, 2000). The result of this is the excretion of excess nitrate and nitrite back into the water column, which, combined with high rates of resupply relative to biological uptake, can culminate in HNLC conditions typical of the Southern Ocean.

The Atlantic sector of the Southern Ocean is composed of a series of water masses, each with distinct physical and chemical properties (Boyer et al., 2013), that are constrained by circumpolar fronts with large geostrophic velocities (Nowlin and Klinck, 1986; Orsi et al., 1995). The differing physical and chemical properties create a high degree of zonal variability within the biology, in particular regarding the timing and extent of phytoplankton seasonal blooms (Thomalla et al., 2011). Key physical controls on this variability include sea ice cover and day length, but this is not enough to explain the full range of measured variability. An alternative approach has examined whether the supply mechanisms of iron to the mixed layer differ significantly in their extent, allowing regions like the sub-Antarctic zone (SAZ) to exhibit prolonged summer blooms in comparison to the polar front zone (PFZ) (Thomalla et al., 2011). Tagliabue et al. (2014) postulated that due to weak diapycnal inputs of iron, there must be a heavy reliance on Fe recycling within the mixed layer to meet the iron demand. An alternative hypothesis is that summer storms can sustain mixed-layer biomass through the entrainment of limiting nutrients, particularly in the SAZ (Carranza and Gille, 2015; Nicholson et al., 2016; Swart et al., 2015). As a storm passes through

the SAZ, it deepens the mixed layer accessing the subsurface iron reservoir; the subsequent re-shoaling of this buoyant water fuels surface water phytoplankton growth in a high-light and replenished-nutrient environment. The drivers of the seasonal characteristics of these regions are likely a combination of both factors, with variable dominance in time and space. Regardless, a greater understanding of the iron supply mechanisms and whether they meet the demand for phytoplankton growth over seasonal timescales is required.

This paper aims to test whether the phytoplankton community in the sub-Antarctic zone is seasonally limited by iron availability. This was done through a series of shipboard grow-out nutrient addition incubation experiments that were performed to determine the extent to which the addition of iron at different times of the growing season would relieve the phytoplankton from iron limitation, driving changes in photophysiology, chlorophyll *a* biomass and potential growth rates.

2 Materials and methods

2.1 Oceanographic sampling

The samples and data presented here were obtained during the annual austral summer relief voyage of the South African National Antarctic Expedition 55 (SANAE 55) onboard the *S.A. Agulhas II* to the Atlantic sector of the Southern Ocean as part of the Southern Ocean Seasonal Cycle Experiment III (SOSCEx III, Swart et al., 2012) from 3 December 2015 to 11 February 2016. During the cruise, three long-term (144–168 h) nutrient addition incubation experiments were performed within the sub-Antarctic zone of the Atlantic sector of the Southern Ocean (Fig. 1, Table 1) to determine whether relief from iron limitation drove variable changes in phytoplankton photophysiology and biomass over the growing season. Uncontaminated, whole seawater was collected from 30 to 35 m depth in Teflon-lined, external-closure 12 L Go-Flo samplers deployed on a trace metal clean CTD (conductivity–temperature–depth) rosette system.

2.2 Nutrient addition incubation experiments

Nutrient addition incubation experiments were performed using methods similar to those employed previously in the Southern Ocean (Moore et al., 2007; Nielsdóttir et al., 2012; Ryan-Keogh et al., 2017a) and the high-latitude North Atlantic (Ryan-Keogh et al., 2013). Water for experiments was transferred unscreened into an acid-washed 50 L LDPE carboy (Thermo Scientific) to ensure homogenization; the homogenized water was then redistributed unscreened into 2.4 L polycarbonate bottles (Nalgene) for the experiments. The triplicate initial samples were collected from the same 50 L LDPE carboy. Experiments during the cruise were incubated under two treatments – control and iron addition

Table 1. Locations of experiments conducted during the cruise along with details of the initial set-up conditions.

Experiment	Experiment 1	Experiment 2	Experiment 3
	"Early summer"	"Midsummer"	"Late summer"
Run time (h)	168	168	144
Initiation date	08/12/2015	05/01/2016	08/02/2016
Initiation time (GMT)	07:00	20:00	02:00
Latitude (° S)	−42.693	−42.693	−43.000
Longitude (° E)	8.738	8.737	8.500
Collection depth (m)	30	35	35
Sunrise : sunset (GMT)	03:30–18:30	04:00–19:00	04:40–18:40
Chl a (mg m^{-3})	0.97	0.84	0.90
Nitrate (µM)	10.60	12.80	13.90
Mean in mixed layer	10.41 ± 0.90	12.76 ± 0.39	12.92 ± 0.84
Silicate (µM)	1.46	1.43	1.39
Mean in mixed layer	1.49 ± 0.05	1.41 ± 0.02	0.84 ± 0.13
Phosphate (µM)	0.88	0.76	0.45
Mean in mixed layer	0.77 ± 0.11	0.76 ± 0.06	0.65 ± 0.21
DFe (nM)	0.16	0.17	0.05
Mean in mixed layer	0.22 ± 0.06	0.15 ± 0.003	0.09 ± 0.01
F_v / F_m	0.19 ± 0.06	0.30 ± 0.02	0.26 ± 0.01
σ_{PSII} (nm^{-2})	14.79 ± 2.46	6.45 ± 0.40	7.08 ± 0.48
MLD (m)	33.77	56.96	43.32
Salinity	33.87	33.70	34.11
Temp (°C)	10.80	10.44	10.80
Average MLD PAR (mol photons m^{-2} d^{-1})	18.29 ± 11.51	7.22 ± 7.36	5.60 ± 3.52
% light depth	14.83	11.59	10.66

(2.0 nM FeCl$_3$, "Fe") – at a constant screened (LEE filters) light level of 129.45 µmol quanta m^{-2} s^{-1}. Light levels were determined using a handheld 4π photosynthetically active radiation (PAR) sensor (Biospherical Instruments), and set on a day : night cycle according to in situ sunset : sunrise times. Experiment incubations were conducted as biological replicates with 16 bottles per treatment for each experiment, these were subsampled at set time points for key variables as outlined in the Supplement (Table S1). Temperature was set at the in situ collection temperature for all samples. All bottle tops were externally sealed with film (Parafilm), and bottles were double bagged with clear polyethylene bags to minimize the risk of contamination during the incubation. Subsampling of all experiments occurred at the same time of day as the initial set-up; see Table 1 for initiation times. All incubations were performed within customized Minus40 Specialized Refrigeration™ units, which were fitted with adjustable (intensity and timing) LED strips as well as a thermostat and cooling fan for temperature control.

2.3 chlorophyll a and nutrient analysis

Samples for chlorophyll a (Chl a), 250 mL, were filtered onto GF/F filters and extracted into 90 % acetone for 24 h in the dark at −20 °C, followed by analysis with a fluorometer (TD70; Turner Designs) (Welschmeyer, 1994). Macronu-

trient samples were drawn into 50 mL diluvials and stored at −20 °C until analysis on land. Nitrate + nitrite and silicate were measured using a Lachat Flow Injection Analyser (Egan, 2008; Wolters, 2002), whilst nitrite and phosphate were determined manually by the colorimetric method as specified by Grasshoff et al. (1983). Dissolved iron samples (DFe) were filtered through 0.2 µm cartridge filters (Acropack) equipped with a 0.45 µm pre-filter, drawn into acid-washed 125 mL LDPE bottles (Nalgene, Thermoscientific), acidified with 30 % HCl Suprapur to pH $\sim$ 1.7 (using 2 mL L^{-1} criteria), double bagged and stored at room temperature until analysis on land at the Université de Bretagne Occidentale (UBO), France, using the chemiluminescence–flow injection analyser (CL-FIA) method (Obata et al., 1993; Sarthou et al., 2003). Accuracy and precision of the method were verified by analysis of in-house internal standards and SAFe reference seawater samples (Johnson et al., 2007); the limits of detection were on the order of 10 pM.

2.4 Phytoplankton photosynthetic physiology

Variable chlorophyll fluorescence was measured using a Chelsea Scientific Instruments FastOcean fast repetition rate fluorometer (FRRf) integrated with a FastAct laboratory system. Samples were acclimated in dark bottles at in situ temperatures, and FRRf measurements were blank corrected us-
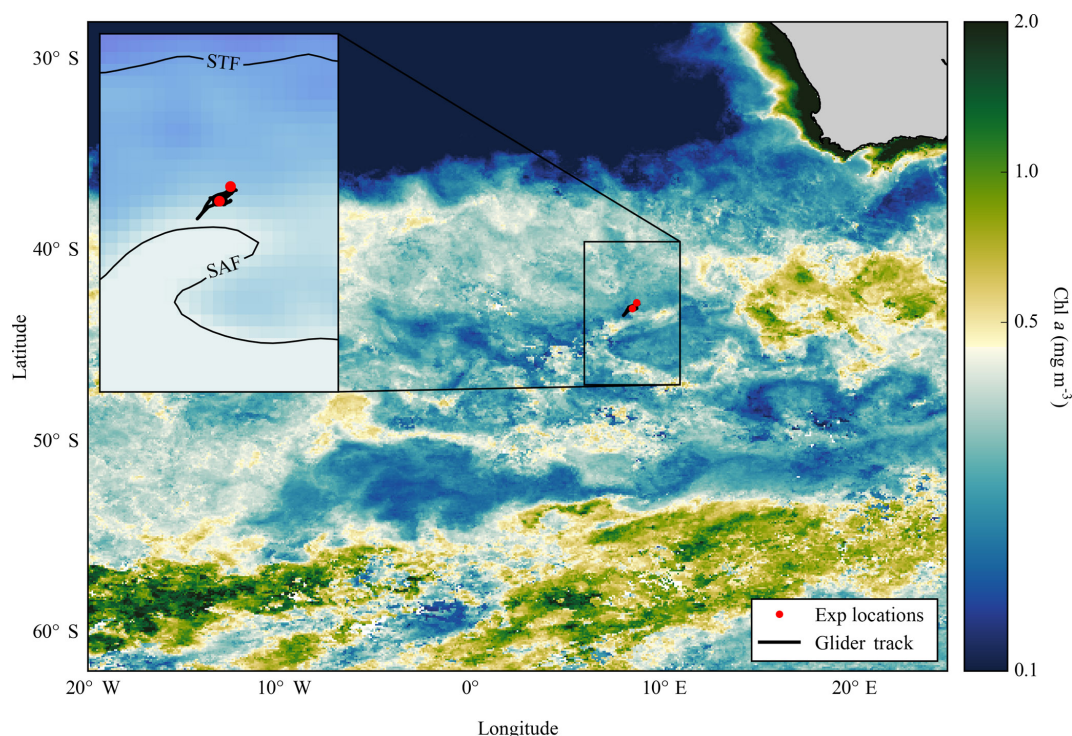
Figure 1. Composite map of MODIS (8 day, 9 km) derived Chl a (mg m^{-3}) from December 2015 to February 2016 for the Atlantic sector of the Southern Ocean, with locations of nutrient addition incubation experiments and the glider track. Inset composite map of absolute dynamic topography (MADT) from the CLS/AVISO product (Rio et al., 2011) from December 2015 to February 2016 with boundary definitions of subtropical front (STF) and sub-Antarctic front (SAF) (Swart et al., 2010), with locations of experiments and glider track.

ing carefully prepared 0.2 µm filtrates for all samples (Cullen and Davis, 2003). FRRf measurements consisted of a single turnover (ST) protocol: 100×2 µs saturation flashlets with a 2 µs interval, followed by 25×1 µs relaxation flashlets with an interval of 84 µs, with a sequence interval of 100 ms. Sequences were repeated 32 times resulting in an acquisition length of 3.2 s. The power of the excitation LED ($\lambda 450$) was adjusted between samples to saturate the observed fluorescence transients within a given range of $R\sigma_{\mathrm{PSII}}$ (the probability of a reaction centre being closed during the first flashlet). $R\sigma_{\mathrm{PSII}}$ was optimized between 0.042 and 0.064 as per manufacturer specifications. By adopting this approach, it ensures the best signal-to-noise ratio in the recovered parameters, whilst accommodating significant variations in the photophysiology of the phytoplankton community without having to adjust the protocol. Data from the FRRf were analysed to derive the fluorescence parameters as defined in Roháček (2002), by fitting transients to the model of Kolber et al. (1998) using the FastPro8 software (v1.0.55).

2.5 Phytoplankton composition

Pigment samples from the incubation experiments were collected by filtering 0.5–2.0 L of water onto 25 mm GF/F filters. Filters were frozen and stored at $-80\,°C$ until analysis in Villefranche, France, on a high-performance liquid

chromatography (HPLC) Agilent Technologies 1200. Filters were extracted in 100 % methanol, disrupted by sonication, clarified by filtration and analysed by HPLC following the methods of Ras et al. (2008); the limits of detection were on the order of 0.1 ng L^{-1}. Pigment composition data were standardized through root square transformation before cluster analysis utilizing multi-dimensional scaling, where similar samples appear together and dissimilar samples do not. Samples were grouped and analysed in CHEMTAX (Mackey et al., 1996) using the Southern Ocean-specific pigment ratios from Gibberd et al. (2013). Multiple iterations of pigment ratios were used to reduce uncertainty in the taxonomic abundance as described in Gibberd et al. (2013), with the solution that had the smallest residual used for the estimated taxonomic abundance.

2.6 Ancillary data

Temperature and salinity profiles were obtained from a Sea-Bird CTD mounted on the rosette system. The mixed-layer depth was calculated following de Boyer Montégut et al. (2004), where the temperature differs from the temperature at 10 m by more than $0.2\,°C$ ($\Delta T_{10\,\mathrm{m}} = 0.2\,°C$). The position of the fronts were determined using sea surface height (SSH) data from maps of absolute dynamic topography (MADT) (Swart et al., 2010). The percentage euphotic

depth was calculated as a function of the natural log of in situ PAR and the diffuse attenuation coefficient K_z.

2.7 Glider dataset

Autonomous Seagliders (SG542 & SG543) were deployed in mooring mode in the sub-Antarctic zone of the Southern Ocean (43° S, 8.5° E) as part of SOSCEx III. SG543 was deployed from 28 July to 8 December 2015, followed by SG542 which continued sampling until 8 February 2016. The deployment of both gliders resulted in a continuous high-resolution time series of 1832 profiles over 196 days, down to depths of 1000 m. The gliders measured a suite of parameters including conductivity, temperature, pressure, PAR, fluorescence and optical backscattering at two wavelengths ($\lambda = 470$ nM and 700 nm). At the deployment and retrieval of each glider, cross-calibration CTD casts were performed (all within 3 km and 4 h of each other), yielding independent inter-calibrations between glider sensors and bottle samples of Chl a. Glider fluorescence was corrected for quenching and converted to units of Chl a (mg m^{-3}), while glider backscattering was de-spiked, smoothed and converted to units of b_{bp} (m^{-1}); for specific details, see Thomalla et al. (2017). The date of the phytoplankton bloom initiation was determined from the integrated Chl a from the mixed layer and euphotic zone when they exceed 5 % of the annual median (Brody et al., 2013; Racault et al., 2012; Siegel et al., 2002; Thomalla et al., 2011). Wind stress (N m^{-2}) data were collected from a weather station mounted on a simultaneous deployment of a Liquid Robotics Wave Glider; wind stress was corrected to 10 m using the wind profile power law (Irwin, 1967).

2.8 Data analysis

Sample means and standard deviations were calculated using Python, followed by tests for normality and equal variance prior to analysis of variance (ANOVA) to determine treatment effects (SciPy v0.17.1, Python v3.6). Significant results are reported at the 95 % confidence level ($p < 0.05$).

3 Results

The experiment set-up location in the SAZ spanned 66 days from the initiation of the first experiment to the initiation of the third experiment. Chlorophyll concentrations did not vary substantially between initiations, ranging from 0.84 to 0.97 mg m^{-3}, alongside no significant variations in temperature or salinity (Table 1). Mean silicate concentrations in the mixed layer were considered limiting and decreased between experiments (1.49–0.84 μM); mean phosphate and DFe also displayed a gradual seasonal depletion (0.77–0.65 μM and 0.22–0.09 nM respectively), whereas mean nitrate concentrations increased throughout the growing season (10.41–12.92 μM) (Table 1). Photophysiological measurements of quantum efficiency (F_v / F_m) ranged from 0.19 to 0.30 (with no seasonal trend) while a seasonal decrease in the cross section of PSII (σ_{PSII}) was observed from 14.79 to 7.08 nm^{-2}. All experiments were set up with water collected from above the mixed layer and the mean euphotic depth of 63.89 ± 19.13 m, with the percentage of surface light ranging from 14.83 to 10.66 %. The bloom initiation date was calculated as 2–3 November for the mixed layer and euphotic zone, with the peak of the bloom calculated as 10–11 December.

Data from 144 to 168 h experiments in the SAZ indicated variable responses to iron addition to the extant phytoplankton community (Fig. 2). During "early summer" (experiment 1), no evidence for iron limitation was observed as indicated in the similar responses in F_v / F_m (Fig. 2a) and chlorophyll (Fig. 2b) between iron addition (+Fe) and control treatments; both variables increased to similar values at the end time point. Statistical analysis confirmed that there were no significant differences in F_v / F_m or chlorophyll throughout experiment 1. The effective cross section of PSII (σ_{PSII} (nm^{-2}), Fig. S1a) displayed a similar pattern with no significant differences between treatments, decreasing in both treatments to 5.68 ± 0.27 and 5.63 ± 0.13 for the control and iron addition treatments respectively. Experiment 2, initiated 28 days later in "midsummer", exhibited signs of iron limitation (Fig. 2c, d) with an increase in F_v / F_m from 0.30 ± 0.02 to a maximum of 0.39 ± 0.01 at 120 h in the +Fe treatment, whilst the control ranged between 0.27 and 0.34 (Fig. 2c). Moreover, Chl a concentrations were >2 times higher in the iron addition treatment compared to the control at the end time point (Fig. 2d). Significant differences were observed for F_v / F_m from 72 h onwards and for Chl a concentrations from 120 h onwards. σ_{PSII} decreased to a minimum of 4.62 ± 0.15 nm^{-2} in the iron addition treatment at 120 h (Fig. S1c), corresponding to the highest value in F_v / F_m, whereas the control treatment decreased from 6.45 ± 0.23 to 5.96 ± 0.13 nm^{-2}. The final experiment in "late summer" (experiment 3) displayed similar evidence for potential iron limitation within the extant phytoplankton community (Fig. 2e, f). F_v / F_m in the control treatment remained constant at 0.26 ± 0.01, whereas in the iron addition treatment it increased to 0.33 ± 0.01 (Fig. 2e). Chl a concentrations were 2.5 times higher in the iron addition treatment compared to the controls after 144 h (Fig. 2f), resulting in significant differences in F_v / F_m from 24 h onwards. σ_{PSII} also decreased to a greater extent than the control in experiment 3: from 7.08 ± 0.48 nm^{-2} to a minimum of 5.45 ± 0.15 nm^{-2} compared to 6.23 ± 0.14 nm^{-2} in the control at 144 h (Fig. S1e).

Chl-a-specific growth rates (μ^{Chl}) were calculated for each experiment (Table 2, Fig. S1b, d, f), displaying significantly higher growth rates for the iron addition treatment in experiments 2 and 3 by up to 50 and 63 % respectively, with no significant differences in experiment 1. Enhanced nitrate drawdown $\Delta(NO_3^-)$ was exhibited in experiment 2 (Table 2), with rates approximately 4 times higher than the other exper-
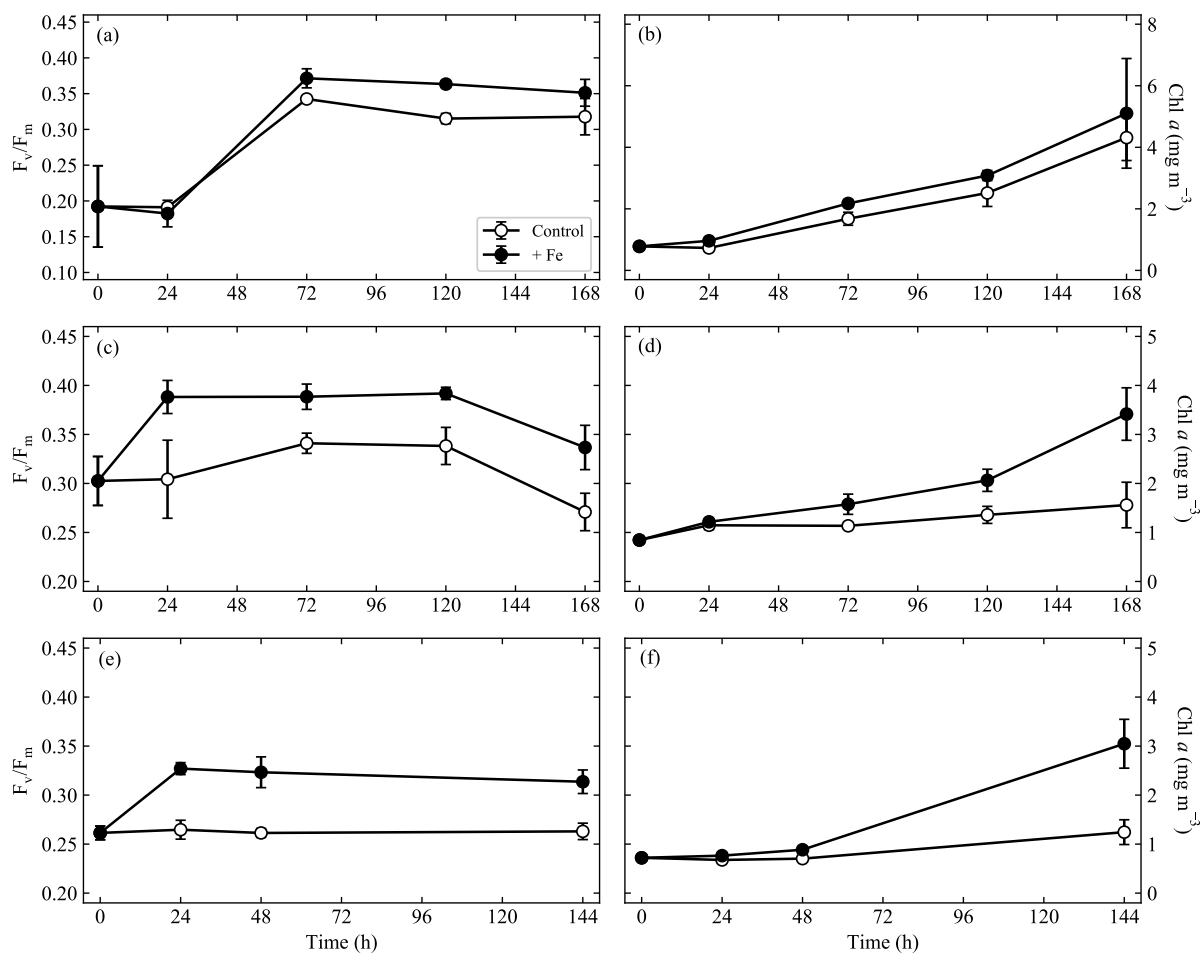
Figure 2. F_v / F_m **(a, c, e)** and chlorophyll a (Chl a) responses (mg m^{-3}) **(b, d, f)**, from the control and Fe addition treatments of experiments initiated in the sub-Antarctic zone over early summer **(a, b)**, midsummer **(c, d)** and late summer **(e, f)**. Displayed here are averages with ±standard deviations ($n = 3 - 5$ for all time points, except the end time point where $n = 6 - 12$; see Table S1 for exact sample numbers). Please note the different scales in panels **(a)** and **(b)**.

iments. No enhanced drawdown of phosphate or silicate was exhibited in any of the experiments. Taxonomic abundance (Fig. S2), indicated that the dominant component of the community was haptophytes (>40 %) when all experiments were initiated. Experiment 1 displayed significant increases in diatoms in both treatments, alongside a significant increase in *Synechococcus* in the control treatment. Experiments 2 and 3 displayed similar results with significant increases in diatoms but only following iron addition, with reductions in the haptophyte group.

F_v / F_m is derived from measurements and analysis of the fluorescence kinetics of the photosynthetic reaction centre photosystem II (PSII) and associated light-harvesting antenna proteins (Kolber and Falkowski, 1993). Understanding the mechanistic changes in F_v / F_m can provide information on how the phytoplankton community respond to different stress factors. Increases in F_v / F_m following iron enrichment do not appear to be the result of an increase in PSII efficiency

Table 2. Net growth rates calculated from Chl a accumulation (μ^{Chl}) and nitrate drawdown ($\Delta(NO_3^-)$) over the full experimental running time ($t = 168, 168, 144$ h). Shown are averages with ±standard deviations, where $n = 6 - 12$ for Chl a and $n = 6 - 7$ for nitrate (see Table S1 for specific details).

Experiment	μ^{Chl} (d^{-1}) 0 – end		$\Delta(NO_3^-)$ (μmol L^{-1} d^{-1})	
	+Fe	Control	+Fe	Control
1	0.28 ± 0.02	0.27 ± 0.02	0.98 ± 0.005	0.82 ± 0.07
2	0.23 ± 0.01	0.11 ± 0.01	4.29 ± 0.43	3.19 ± 0.54
3	0.23 ± 0.01	0.09 ± 0.01	0.78 ± 0.11	0.91 ± 0.15

(F_v) but rather are due to decreases in F_m and F_o (Behrenfeld et al., 2006; Lin et al., 2016; Macey et al., 2014; Ryan-Keogh et al., 2017a). To determine these relative changes in photophysiology, the absolute difference in F_v / F_m between the control and iron addition bottles was calculated at 24 h,

$\Delta(F_v / F_m)$ (Ryan-Keogh et al., 2013). $\Delta(F_v / F_m)$ in experiment 1 was indistinguishable from zero (Fig. 3a), whereas in experiment 2 and 3 it was consistently positive with values of 0.08 ± 0.01 and 0.06 ± 0.00 respectively. These responses were markedly similar to the absolute differences in growth rates (Fig. 3b), with significantly higher differences in experiments 2 and 3. The absolute changes in maximum fluorescence (F_m, Fig. 3c) and variable fluorescence (F_v, Fig. 3d) normalized to chlorophyll were calculated to determine the mechanistic response. Significant differences were determined for F_m Chl^{-1} in experiments 2 and 3, with no significant differences in F_v Chl^{-1} across any experiments.

4 Discussion

Photosynthesis in the Southern Ocean is considered to be limited in winter by low mean irradiance, with net phytoplankton growth rates increasing rapidly following the onset of stratification in spring (Sverdrup, 1953). Despite these high levels of productivity and growth, complete macronutrient drawdown is not possible due primarily to constraints in the availability of iron (Boyd et al., 2007; de Baar et al., 1990). Reasons for this growth limitation include the high iron requirements of the photosynthetic apparatus (Raven, 1990; Raven et al., 1999; Shi et al., 2007; Strzepek and Harrison, 2004) particularly under low-light conditions and a lack of iron sources (Duce and Tindale, 1991; Tagliabue et al., 2014). Phytoplankton blooms in the SAZ are characterized by high inter-annual and intra-seasonal variability with an extended duration that sustains high chlorophyll concentrations late into summer (Carranza and Gille, 2015; Racault et al., 2012; Swart et al., 2015; Thomalla et al., 2011, 2015). The longevity of these late summer blooms is unusual as iron limitation at this time of year is expected to be limiting growth (Boyd, 2002). To determine the extent to which seasonal variability in the availability of iron restricts phytoplankton photosynthesis and biomass accumulation in the SAZ, a series of grow-out nutrient addition incubation experiments were performed during the austral summer of 2015–2016.

The nutrient addition experiments (Fig. 2) demonstrated the development of seasonal iron limitation of the in situ phytoplankton population within the SAZ from early summer (December) to late summer (February). Experiment 1, which was set up during the peak of the bloom did not display any significant differences between control and +Fe treatments, indicative of a system in which the iron supply was sufficient to meet community needs, driving maximum potential growth rates (Fig. 2a, b). The rapid increase in F_v / F_m observed in both treatments from 24 h onwards is likely a response to potential bottle effects in particular with respect to a change in the light environment (Coale, 1991; de Baar et al., 1990, 2005; Martin and Fitzwater, 1988). The total daily PAR in the incubators ranged from 6.52 to 6.99 mol pho-

tons m^{-2} d^{-1}, which is similar to the in situ light environments of experiments 2 and 3. However, this was a $\sim 62\%$ decrease in the daily PAR that the phytoplankton community in experiment 1 was previously subjected to. Such a decrease in PAR would be expected to lead to a decrease in the downregulation of PSII by photodamage, coincident with an anticipated response in community structure. This could explain the observed increase in F_v / F_m and σ_{PSII} as larger cells tend to have a higher F_v / F_m and small σ_{PSII} in comparison to smaller cells (Suggett et al., 2009). Indeed, we did observe a change in the community structure for experiment 1 (Fig. S2), suggestive of the fact that a decrease in light pressure resulted in a community response in the control treatment. However, the lack of taxonomic data at 72 h makes it difficult to distinguish whether the primary driver of this response is physiological, taxonomic or a combination of both. When examining the photophysiology alone, experiment 2 displayed the greatest response to iron addition (Fig. 2c) with significant responses also observed in Chl-a-derived net growth rates (Fig. S1) and nitrate drawdown rates (Table 2). Experiment 3 displayed the greatest increases in growth rates following Fe addition (Fig. S1, Table 2), while significantly higher F_v / F_m was similarly observed (Fig. 2e). The addition of iron also resulted in changes at the community level, switching from haptophyte- to diatom-dominated communities (Fig. S2) despite apparent silica limitation (1.49–0.84 μM), typical of the region (Boyd et al., 2010; Hutchins et al., 2001). This suggests a switch to smaller diatoms, which have lower silica requirements than larger ones (Hutchins et al., 2001). Regardless, this community shift is suggestive of community-specific iron quota requirements (Ryan-Keogh et al., 2017a; Strzepek et al., 2011, 2012), which drive the composition of the extant phytoplankton community in the SAZ.

Mechanistic changes in F_v / F_m, i.e. $\Delta(F_v / F_m)$, are a useful proxy to determine the potential physiological signal of iron limitation without any superimposing taxonomic signal (Suggett et al., 2009). The derived variable $\Delta(F_v / F_m)$ was higher in experiments in 2 and 3 (Fig. 3a), with values consistent with studies from the North and South Atlantic and the Ross Sea (Browning et al., 2014; Ryan-Keogh et al., 2013, 2017a), which correlated well with the observed differences in net growth rates ($\Delta\mu^{Chl}$, Fig. 3b). Whilst no empirical relationship should be inferred between measures of photophysiology and measures of growth rates (Kruskopf and Flynn, 2006; Parkhill et al., 2001; Price, 2005), the observed correlation between these two independent variables suggests that a biomass-independent measure of physiological iron limitation, F_v / F_m, is likely accompanied by a significant repression of phytoplankton growth rates. These experiments also provide insight into the mechanistic iron-stress response of phytoplankton photophysiology, where increases in F_v / F_m following iron addition are due to a reduction in the ratio of F_m Chl^{-1} rather than F_v Chl^{-1} (Fig. 3c, d). This is in agreement with similar observations made in the Ross Sea, the high-latitude North Atlantic and the equato-

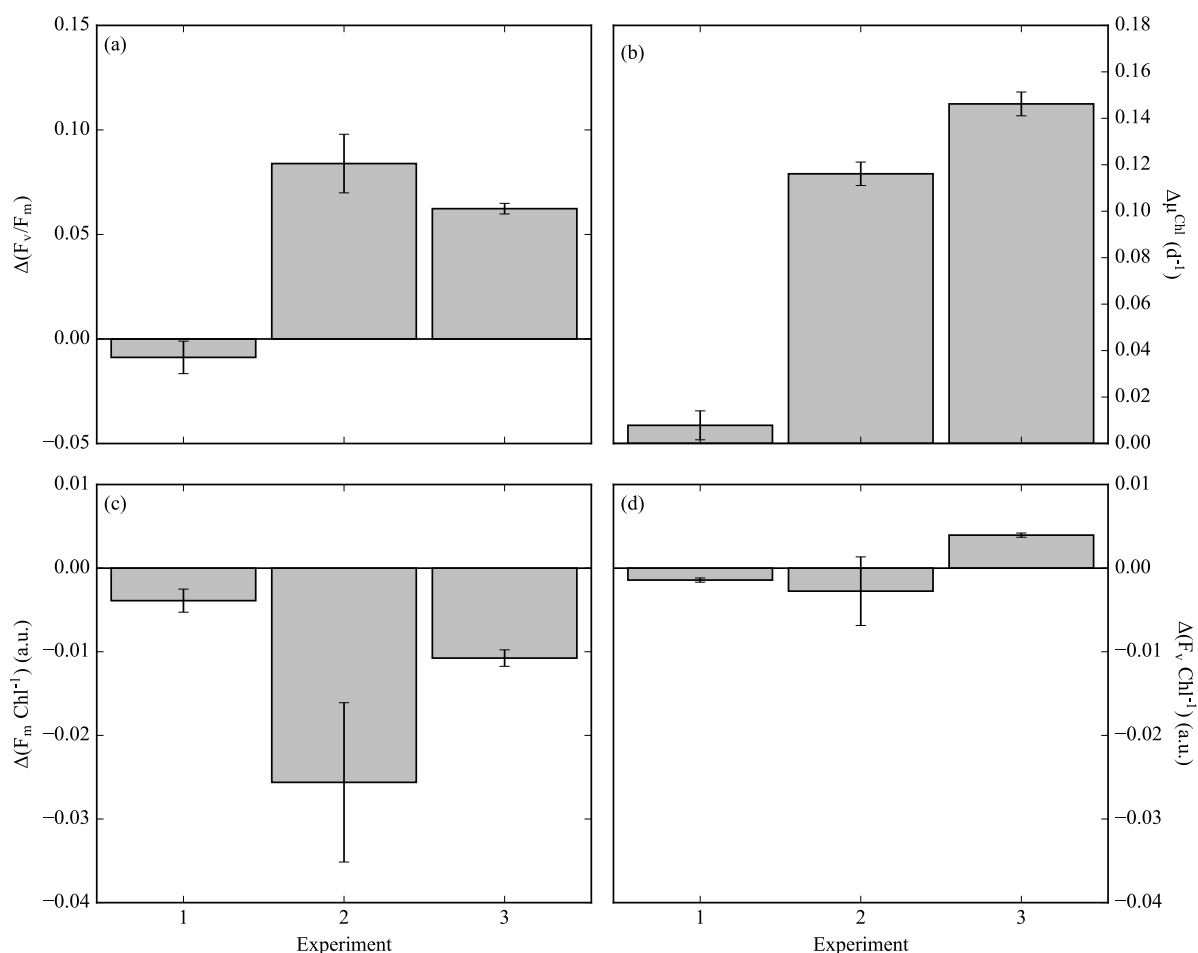**Figure 3. (a)** The difference in F_v / F_m between the Fe treatment and control treatment ($\Delta(F_v / F_m)$) at the 24 h time point for experiments initiated in early summer (experiment 1), midsummer (experiment 2) and late summer (experiment 3), where ($n = 3$ for $\Delta(F_v / F_m)$). **(b)** The difference in chlorophyll-derived net growth rates ($\Delta\mu^{Chl}(d^{-1})$), where $t = 168$, 168 and 144 h. **(c)** The change in chlorophyll normalized maximum fluorescence, ($\Delta F_m \, Chl^{-1}$). **(d)** The change in chlorophyll normalized variable fluorescence, ($\Delta F_v \, Chl^{-1}$). Displayed here are averages with ±standard deviations ($n = 6$ for experiment 1, 10 for experiment 2 and 12 for experiment 3).

rial Pacific (Behrenfeld et al., 2006; Lin et al., 2016; Macey et al., 2014; Ryan-Keogh et al., 2017a), all regions where the phytoplankton communities are subject to iron limitation. Elevated ratios of $F_m \, Chl^{-1}$ are potentially indicative of an energetically decoupled pool of chlorophyll that possesses a higher fluorescence yield than PSII at F_m (Macey et al., 2014; Ryan-Keogh et al., 2012, 2017a; Schrader et al., 2011). These pools can be significant in iron-limited regions with important implications for Chl-*a*-derived primary productivity estimates that can be overestimated as a result (Behrenfeld et al., 2006; Macey et al., 2014). These results all confirm physiological evidence of community level iron limitation from midsummer to late summer, after the peak of the bloom as determined from the glider time series.

The transition from no response in experiment 1 to an increased response in experiments 2 and 3 is indicative of an increase in seasonal iron limitation, similar to that observed in the high-latitude North Atlantic (Ryan-Keogh et al., 2013), where available iron is depleted early in the growing season and additional resupply is insufficient to meet biological demands during the latter parts of the growing season, driving characteristic HNLC conditions. A progressive decrease in ambient iron concentrations (mean in the mixed layer; Table 1) in the SAZ are also suggestive of a seasonal progression of iron limitation. However, it is worth bearing in mind that nutrient concentrations are often a poor indicator of iron limitation, as any limiting nutrient would be expected to be severely depleted through biological uptake with resultant ambient concentrations that remain close to zero despite possible event-scale supply (Ryan-Keogh et al., 2017a).

The seasonal development of iron limitation in the SAZ after the peak of the bloom is suggestive of a primary dominant iron source to the surface waters: winter entrainment, which is subsequently depleted by upper-ocean biota and
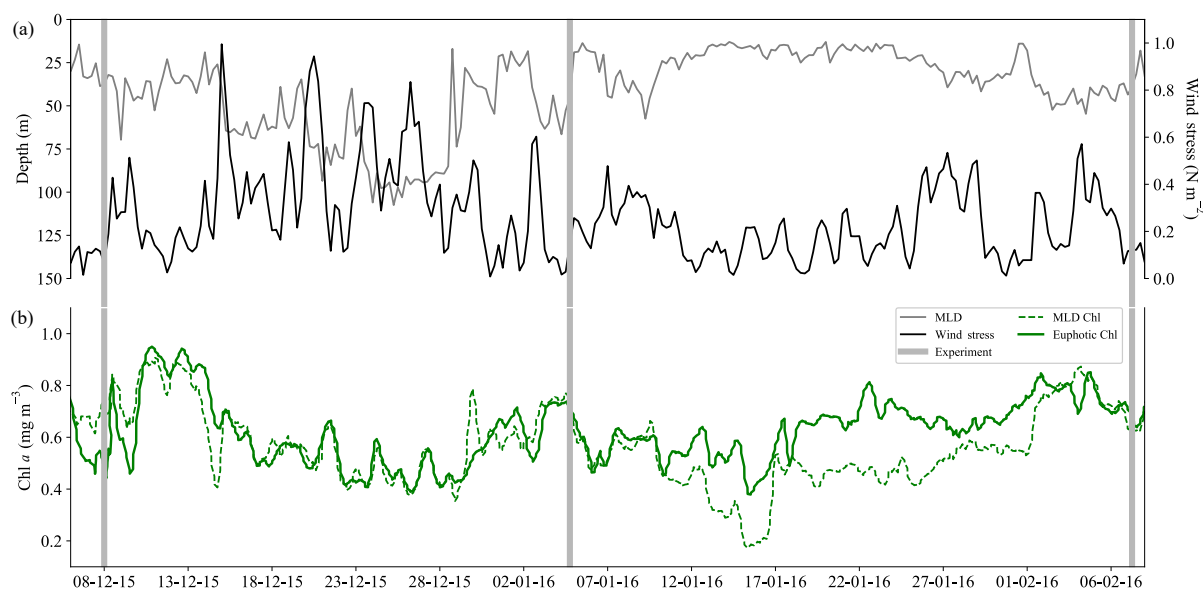
Figure 4. Time series from 6 December 2015 to 8 February 2016 of **(a)** surface wind stress ($\mathrm{N\,m^{-2}}$), mixed-layer depth (MLD; m) where $\Delta T_{10\,\mathrm{m}} = 0.2\,^{\circ}\mathrm{C}$, and **(b)** mean Chl a concentration ($\mathrm{mg\,m^{-3}}$) from the MLD and the euphotic zone. Experiment initiation dates are overlaid in grey bars.

abiotic scavenging onto settling particles (Tagliabue et al., 2014). Although diapycnal diffusion resupplies the mixed layer from late spring onwards, its low rates cannot be reconciled with potential phytoplankton uptake (Tagliabue et al., 2014). Instead, Tagliabue et al. (2014) propose that biologically recycled iron within the mixed layer is the dominant mechanism for sustaining summertime blooms. However, there is now compelling evidence to suggest that storm events may also play a critical role in extending the duration of summertime production through intra-seasonal entrainment of dissolved iron from a subsurface reservoir (Carranza and Gille, 2015; Fauchereau et al., 2011; Swart et al., 2015; Thomalla et al., 2011). This mechanism was tested using a 1-D biogeochemical model by Nicholson et al. (2016) whose results suggest that intra-seasonal mixed-layer perturbations may offer relief from iron limitation in summer, particularly if there is sufficient subsurface vertical mixing beneath the surface mixed layer.

A SAZ glider study by Little et al. (2018) corroborated these findings with summer matchups in small-scale temporal variability (<10 days) in wind stress, mixed-layer depth (MLD) and chlorophyll that emphasizes the interconnectedness between physical drivers and their biological response. Despite the similarity in the scales of variability, no correlation was observed between MLD and Chl a, which is explained by the variable response that MLD adjustments drive, i.e. dilution (a decrease in Chl a with increasing MLD) and growth (an increase in Chl a with increasing MLD in response to nutrient entrainment) (Fauchereau et al., 2011). Both of these scenarios can be observed in the glider time series from this study (Fig. 4), where increased wind stress and deeper MLDs were associated with both reduced (15–29 December) and enhanced (29 January–7 February) Chl a. The midsummer to late summer experiments were set up during periods of low wind stress ($<0.2\,\mathrm{N\,m^{-2}}$) with shallow MLDs, which may corroborate the positive response to iron relief observed in experiments 2 and 3. Worth noting is that the time period between 10 and 29 January is when the SAZ experienced uncharacteristically low winds (Braun, 2008) for an extended period of time, driving shallow MLDs ($\sim 20\,\mathrm{m}$) and the development of subsurface Chl a (Fig. S3a), indicative of iron limitation within the mixed layer and a supply mechanism (seasonal, sub-seasonal, remineralized or storm-driven) that is not sufficient to meet mixed-layer phytoplankton demands. Precaution must, however, be taken when investigating Chl a concentration as a proxy for phytoplankton biomass (Behrenfeld et al., 2016; Bellacicco et al., 2016; Mignot et al., 2014; Westberry et al., 2008, 2016), as a higher average concentration over the euphotic zone ($0.8\,\mathrm{mg\,m^{-3}}$) relative to the shallower mixed layer ($0.4\,\mathrm{mg\,m^{-3}}$) may represent a Chl a packaging effect due to lower light levels at depth (rather than an increase in biomass). As such, particulate backscatter (b_{bp}) (Fig. S3b) was investigated as an alternate proxy for phytoplankton biomass (Loisel et al., 2002; Stramski et al., 1999), which similarly depicted the presence of a subsurface bloom in response to anticipated iron relief at depth.

What is potentially hard to reconcile with sustained seasonal productivity and a seasonal decrease in phosphate, silicate and DFe is the observed increase in nitrate. However,

this too is suggestive of community level iron limitation, as iron limitation can reduce the availability of photosynthetic reductant for nitrate reduction which can lead to the excretion of excess nitrate back into the water column (Cochlan, 2008; Lucas et al., 2007; Milligan and Harrison, 2000; Moore et al., 2013; Price et al., 1994). This, together with the likely resupply of nitrate from below the mixed layer via sub-seasonal storm events, which is not accessible to phytoplankton uptake due to iron limitation of nitrate reductase, could account for the observed seasonal increase in mixed-layer nitrate. Irrespective of the different supply mechanisms (winter entrainment, storm-driven entrainment, diapycnal diffusion, photochemical reduction or microbial regeneration), the iron supply to the mixed layer over midsummer to late summer is not sufficient for phytoplankton to reach maximum growth potential and completely draw down all available macronutrients. Moreover, this seasonal iron limitation may not be the only cause of sub-maximal productivity rates as silicate can also potentially limit phytoplankton growth in this region (Boyd et al., 2010; Hutchins et al., 2001). However, the significant shifts to diatom from haptophyte communities (Fig. S2) within the experimental treatments following iron addition suggest that silicate limitation may only be a secondary limiting factor.

Although the Southern Ocean is known to be an iron-limited HNLC region, this is the first study to investigate the seasonal progression of iron limitation in the sub-Antarctic zone. Results suggest that the system is not limited by iron in early summer, as evidenced by the lack of response in experiment 1, which implies that winter entrainment was sufficient to meet phytoplankton community demands. Although the sub-seasonal supply of iron, regardless of the mechanism proposed, appears to play an important role in sustaining the seasonal bloom, it is insufficient to meet the demands of the community as evidenced by the increased photosynthetic efficiency, growth rates and nutrient drawdown in experiments 2 and 3. This is important for understanding iron demand by the biota given the climate-mediated variability in supply mechanisms (i.e. atmospheric deposition, Mackie et al., 2008), mixed-layer depths and sea-ice cover (Boyd et al., 2012), as well as phytoplankton phenology (Strzepek et al., 2012). The biogeochemical significance of the Southern Ocean, including the highly productive Atlantic sector, will increase with respect to climate change (Marinov et al., 2006), particularly as the Southern Ocean is a HNLC region where the cryosphere is critical to seasonal dynamics (Massom and Stammerjohn, 2010). Climate-mediated changes to iron supply will thus influence the overall extent of phytoplankton growth, macronutrient drawdown and ultimately the strength and efficiency of the biological carbon pump. However, the variations in supply in the seasonal cycle will also continue to play an important role in this ecologically important oceanic region and warrant further investigation.

References

Behrenfeld, M. J., Worthington, K., Sherrell, R. M., Chavez, F. P., Strutton, P., McPhaden, M., and Shea, D. M.: Controls on tropical Pacific Ocean productivity revealed through nutrient stress diagnostics, Nature, 442, 1025–1028, https://doi.org/10.1038/nature05083, 2006.

Behrenfeld, M. J., O'Malley, R. T., Boss, E. S., Westberry, T. K., Graff, J. R., Halsey, K. H., Milligan, A. J., Siegel, D. A., and Brown, M. B.: Reevaluating ocean warming impacts on global phytoplankton, Nat. Clim. Change, 6, 323–330, https://doi.org/10.1038/nclimate2838, 2016.

Bellacicco, M., Volpe, G., Colella, S., Pitarch, J., and Santoleri, R.: Influence of photoacclimation on the phytoplankton seasonal cycle in the Mediterranean Sea as seen by satellite, Remote Sens. Environ., 184, 595–604, https://doi.org/10.1016/j.rse.2016.08.004, 2016.

Bopp, L., Aumont, O., Cadule, P., Alvain, S., and Gehlen, M.: Response of diatoms distribution to global warming and potential implications: A global model study, Geophys. Res. Lett., 32, L19606, https://doi.org/10.1029/2005GL023653, 2005.

Boyd, P. W.: Environmental factors controlling phytoplankton processes in the Southern Ocean, J. Phycol., 38, 844–861, https://doi.org/10.1046/j.1529-8817.2002.t01-1-01203.x, 2002.

Boyd, P. W., Jickells, T., Law, C. S., Blain, S., Boyle, E. A., Buesseler, K. O., Coale, K. H., Cullen, J. J., de Baar, H. J. W., Follows, M., Harvey, M., Lancelot, C., Levasseur, M., Owens, N. P. J., Pollard, R., Rivkin, R. B., Sarmiento, J., Schoemann, V., Smetacek, V., Takeda, S., Tsuda, A., Turner, S., and Watson, A. J.: Mesoscale iron enrichment experiments 1993–2005: Synthesis and future directions, Science, 315, 612–617, https://doi.org/10.1126/science.1131669, 2007.

Boyd, P. W., Strzepek, R., Fu, F. X., and Hutchins, D. A.: Environmental control of open-ocean phytoplankton groups: Now and in the future, Limnol. Oceanogr., 55, 1353–1376, https://doi.org/10.4319/lo.2010.55.3.1353, 2010.

Boyd, P. W., Arrigo, K. R., Strzepek, R., and van Dijken, G. L.: Mapping phytoplankton iron utilization: Insights into Southern Ocean supply mechanisms, J. Geophys. Res., 117, C06009, https://doi.org/10.1029/2011JC007726, 2012.

Boyer, T. P., Antonov, J. I., Baranova, O. K., Coleman, C., Garcia, H. E., Grodsky, A., Johnson, D. R., Locarnini, R. A., Mishonov, A. V., and O'Brien, T. D.: World Ocean Database 2013, NOAA Printing Office, Silver Spring, Maryland, USA, 2013.

Braun, A. V.: A comparison of subtropical storms in the South Atlantic basin with Australian east-coast cyclones, 28th Conference on Hurricanes and Tropical Meteorology, 5, 2008.

Brody, S. R., Lozier, M. S., and Dunne, J. P.: A comparison of methods to determine phytoplankton bloom initiation, J. Geophys. Res., 118, 2345–2357, https://doi.org/10.1002/jgrc.20167, 2013.

Browning, T. J., Bouman, H. A., Moore, C. M., Schlosser, C., Tarran, G. A., Woodward, E. M. S., and Henderson, G. M.: Nutrient regimes control phytoplankton ecophysiology in the South Atlantic, Biogeosciences, 11, 463–479, https://doi.org/10.5194/bg-11-463-2014, 2014

Carranza, M. M. and Gille, S. T.: Southern Ocean wind-driven entrainment enhances satellite chlorophyll-a through the summer, J. Geophys. Res.-Oceans, 120, 304–323, https://doi.org/10.1002/2014JC010203, 2015.

Coale, K. H.: Effects of iron, manganese, copper, and zinc enrichments on productivity and biomass in the subarctic Pacific, Limnol. Oceanogr., 36, 1851–1864, https://doi.org/10.4319/lo.1991.36.8.1851, 1991.

Cochlan, W. P.: Nitrogen Uptake in the Southern Ocean, in: Nitrogen in the Marine Environment, Elsevier, Amsterdam, 2008.

Cullen, J. J. and Davis, R. F.: The blank can make a big difference in oceanographic measurements, Limnol. Oceanogr., 12, 29–35, https://doi.org/10.1002/lob.200312229, 2003.

de Baar, H. J. W., Buma, A. G. J., Nolting, R. F., Cadee, G. C., Jacques, G., and Treguer, P. J.: On iron limitation of the Southern Ocean: Experimental observations in the Weddell and Scotia Seas, Mar. Ecol. Prog. Ser., 65, 105–122, https://doi.org/10.3354/meps065105, 1990.

de Baar, H. J. W., Boyd, P. W., Coale, K. H., Landry, M. R., Tsuda, A., Assmy, P., Bakker, D. C. E., Bozec, Y., Barber, R. T., Brezinski, M. A., Buesseler, K. O., Boyé, M., Croot, P. L., Gervais, F., Gorbunov, M. Y., Harrison, P. J., Hiscock, W. T., Laan, P., Lancelot, C., Law, C. S., Levasseur, M., Marchetti, A., Millero, F. J., Nishioka, J., Nojiri, Y., van Oijen, T., Riebesell, U., Rijkenberg, M. J. A., Saito, H., Takeda, S., Timmermans, K. R., Veldhuis, M. J. W., Waite, A. M., and Wong, C. S.: Synthesis of iron fertilization experiments: From the iron age in the age of enlightenment, J. Geophys. Res., 110, C09S16, https://doi.org/10.1029/2004JC002601, 2005.

de Boyer Montégut, C., Madec, G., Fischer, A. S., Lazar, A., and Iudicone, D.: Mixed layer depth over the global ocean: an examination of profile data and a profile-based climatology, J. Geophys. Res., 109, C12003, https://doi.org/10.1029/2004JC002378, 2004.

Dubischar, C. D. and Bathmann, U. V.: Grazing impacts of copepods and salps on phytoplankton in the Atlantic sector of the Southern Ocean, Deep.-Sea. Res. Pt. 1, 44, 415–433, https://doi.org/10.1016/S0967-0645(96)00064-1, 1997.

Duce, R. A. and Tindale, N. W.: Atmospheric Transport of Iron and Its Deposition in the Ocean, Limnol. Oceanogr., 36, 1715–1726, https://doi.org/10.4319/lo.1991.36.8.1715, 1991.

Egan, L.: QuickChem Method 31-107-04-1-C – Nitrate and/or Nitrite in brackish or seawater, Lachat Instruments, Colorado, USA, 2008.

Fauchereau, N., Tagliabue, A., Bopp, L., and Monteiro, P. M. S.: The response of phytoplankton biomass to transient mixing events in the Southern Ocean, Geophys. Res. Lett., 38, L17601, https://doi.org/10.1029/2011GL048498, 2011.

Gibberd, M.-J., Kean, E., Barlow, R., Thomalla, S., and Lucas, M.: Phytoplankton chemotaxonomy in the Atlantic sector of the Southern Ocean during late summer 2009, Deep.-Sea. Res. Pt. 1, 78, 70–78, https://doi.org/10.1016/j.dsr.2013.04.007, 2013.

Grasshoff, K., Ehrhardt, M., and Kremling, K.: Methods of seawater analysis, Verlag Chemie, Wienheim, Germany, 1983.

Hiscock, M. R., Lance, V. P., Apprill, A. M., Johnson, Z., Bidigare, R. R., Mitchell, B. G., Smith, W. O. J., and Barber, R. T.: Photosynthetic maximum quantum yield increases are an essential component of Southern Ocean phytoplankton iron response, P. Natl. Acad. Sci. USA, 105, 4775–4780, https://doi.org/10.1073/pnas.0705006105, 2008.

Hutchins, D. A., Sedwick, P. N., DiTullio, G. R., Boyd, P. W., Quéguiner, B., Griffiths, F. B., and Crossely, C.: Control of phytoplankton growth by iron and silicic acid availability in the subantarctic Southern Ocean: Experimental results from the SAZ Project, J. Geophys. Res., 106, 31559–31572, https://doi.org/10.1029/2000JC000333, 2001.

Irwin, J. S.: A theoretical variation of the wind profile power-law exponent as a function of surface roughness and stability, Atmos. Environ., 13, 191–194, https://doi.org/10.1016/0004-6981(79)90260-9, 1967.

Johnson, K. S., Elrod, V. A., Fitzwater, S. E., Plant, J., Boyle, E., Bergquist, B., Bruland, K. W., Aguilar-Islas, A. M., Buck, K., Lohan, M. C., Smith, G. J., Sohst, B. M., Coale, K. H., Gordon, M., Tanner, S., Measures, C. I., Moffett, J., Barbeau, K. A., King, A., Bowie, A. R., Chase, Z., Cullen, J. J., Laan, P., Landing, W., Mendez, J., Milne, A., Obata, H., Doi, T., Ossiander, L., Sarthou, G., Sedwick, P. N., Van den Berg, S., Laglera-Baquer, L., Wu, J.-F., and Cai, Y.: Developing standards for dissolved iron in seawater, Eos, Transactions American Geophysical Union, 88, 131–132, https://doi.org/10.1029/2007EO110003, 2007.

Khatiwala, S., Primeua, F., and Hall, T.: Reconstruction of the history of anthropogenic CO_2 concentrations in the ocean, Nature, 462, 346–349, https://doi.org/10.1038/nature08526, 2009.

Kolber, Z. S. and Falkowski, P. G.: Use of active fluorescence to estimate phytoplankton photosynthesis in situ, Limnol. Oceanogr.,

38, 1646–1665, https://doi.org/10.4319/lo.1993.38.8.1646, 1993.

Kolber, Z. S., Prášil, O., and Falkowski, P. G.: Measurements of variable chlorophyll fluorescence using fast repetition rate techniques: defining methodology and experimental protocols, Biochim. Biophys. Acta., 1367, 88–106, https://doi.org/10.1016/S0005-2728(98)00135-2, 1998.

Kruskopf, M. and Flynn, K. J.: Chlorophyll content and fluorescence responses cannot be used to gauge reliably phytoplankton biomass, nutrient status or growth rate, New. Phytol., 169, 525–536, https://doi.org/10.1111/j.1469-8137.2005.01601.x, 2006.

Le Quéré, C., Raupach, M. R., Canadell, J. G., Marland, G., Bopp, L., Ciais, P., Conway, T. J., Doney, S. C., Feely, R. A., Foster, P., Friendlingstein, P., Gurney, K., Houghton, R. A., House, J. I., Huntingford, C., Levy, P. E., Lomas, M. R., Majkut, J., Metzl, N., Ometto, J. P., Peters, G. P., Prentice, I. C., Randerson, J. T., Running, S. W., Sarmiento, J. L., Schuster, U., Sitch, S., Takahashi, T., Viovy, N., van der Werf, G. R., and Woodward, F. I.: Trends in the sources and sinks of carbon dioxide, Nat. Geosci., 2, 831–836, https://doi.org/10.1038/ngeo689, 2009.

Lin, H., Kuzimov, F. I., Park, J., Lee, S., Falkowski, P. G., and Gorbunov, M. Y.: The fate of photons absorbed by phytoplankton in the global ocean, Science, 351, 264–267, https://doi.org/10.1126/science.aab2213, 2016.

Little, H., Vichi, M., Thomalla, S. J., and Swart, S.: Spatial and temporal scales of chlorophyll variability using high-resolution glider data, J. Marine Syst., 187, 1–12, https://doi.org/10.1016/j.marsys.2018.06.011, 2018.

Loisel, H., Nicolas, J. M., Deschamps, P. Y., and Frouin, R.: Seasonal and inter-annual variability of particulate organic matter in the global ocean, Geophys. Res. Lett., 29, 2196, https://doi.org/10.1029/2002GL015948, 2002.

Lucas, M., Seeyave, S., Sanders, R., Moore, C. M., Williamson, R., and Stinchcombe, M.: Nitrogen uptake responses to a naturally Fe-fertilised phytoplankton bloom during the 2004/2005 CROZEX study, Deep.-Sea. Res. Pt. 1, 54, 2138–2173, https://doi.org/10.4319/lo.2007.52.6.2540, 2007.

Macey, A. I., Ryan-Keogh, T. J., Richier, S., Moore, C. M., and Bibby, T. S.: Photosynthetic protein stoichiometry and photophysiology in the high latitude North Atlantic, Limnol. Oceanogr., 59, 1853–1864, https://doi.org/10.4319/lo.2014.59.6.1853, 2014.

Mackey, M. D., Mackey, D. J., Higgins, H. W., and Wright, S. W.: CHEMTAX – a program for estimating class abundances from chemical markers: application to HPLC measurements of phytoplankton, Mar. Ecol. Prog. Ser., 144, 265–283, https://doi.org/10.3354/meps144265, 1996.

Mackie, D. S., Boyd, P. W., McTainsh, G. H., Tindale, N. W., Westberry, T. K., and Hunter, K. A.: Biogeochemistry of iron in Australian dust: From eolian uplift to marine uptake, Geochem. Geophy. Geosy., 9, Q03Q08, https://doi.org/10.1029/2007GC001813, 2008.

Maldonado, M. T., Boyd, P. W., Harrison, P. J., and Price, N. M.: Co-limitation of phytoplankton growth by light and Fe during winter in the NE subarctic Pacific Ocean, Deep.-Sea. Res. Pt. 1, 46, 2475–2485, https://doi.org/10.1016/S0967-0645(99)00072-7, 1999.

Marinov, I., Gnanadesikan, A., Toggweiler, J. R., and Sarmiento, J. L.: The Southern Ocean biogeochemical divide, Nature, 441, 964–967, https://doi.org/10.1038/nature04883, 2006.

Martin, J. H. and Fitzwater, S. E.: Iron deficiency limits phytoplankton growth in the northeast Pacific subarctic, Nature, 331, 341–343, https://doi.org/10.1038/331341a0, 1988.

Martin, J. H., Gordon, R. M., and Fitzwater, S. E.: Iron in Antarctic waters, Nature, 345, 156–158, https://doi.org/10.1038/345156a0, 1990.

Massom, R. A. and Stammerjohn, S. E.: Antarctic sea ice change and variability – Physical and ecological implications, Polar Sci., 4, 149–186, https://doi.org/10.1016/j.polar.2010.05.001, 2010.

Mignot, A., Claustre, H., Uitz, J., Poteau, A., D'Ortenzio, F., and Xing, X.: Understanding the seasonal dynamics of phytoplankton biomass and the deep chlorophyll maximum in oligotrophic environments: A Bio-Argo float investigation, Global Biogeochem. Cy., 28, 856–876, https://doi.org/10.1002/2013GB004781, 2014.

Mikaloff Fletcher, S. E., Gruber, N., Jacobson, A. R., Doney, S. C., Dutkiewicz, S., Gerber, M., Follows, M., Joos, F., Lindsay, K., Menemenlis, D., Mouchet, A., Müller, S. A., and Sarmiento, J. L.: Inverse estimates of anthropogenic CO_2 uptake, transport, and storage by the ocean, Global Biogeochem. Cy., 20, GB2002, https://doi.org/10.1029/2005GB002530, 2006.

Milligan, A. J. and Harrison, P. J.: Effects of non-steady-state iron limitation on nitrogen assimilatory enzymes in the marine diatom Thalassiosira weissflogii (Bacillariophyceae), J. Phycol., 36, 78–86, https://doi.org/10.1046/j.1529-8817.2000.99013.x, 2000.

Moore, C. M., Seeyave, S., Hickman, A. E., Allen, J. T., Lucas, M. I., Planquette, H., Pollard, R. T., and Poulton, A. J.: Iron-light interactions during the CROZet natural iron bloom and EXport experiment (CROZEX) I: Phytoplankton growth and photophysiology, Deep.-Sea. Res. Pt. 1, 54, 2045–2065, https://doi.org/10.1016/j.dsr2.2007.06.011, 2007.

Moore, C. M., Mills, M. M., Arrigo, K. R., Berman-Frank, I., Bopp, L., Boyd, P. W., Galbraith, E. D., Geider, R. J., Guieu, C., Jaccard, S. L., Jickells, T. D., La Roche, J., Lenton, T. M., Mahowald, N. M., Marañón, E., Marinov, I., Moore, J. K., Nakatsuka, T., Oschlies, A., Saito, M. A., Thingstad, T. F., Tsuda, A., and Ulloa, O.: Processes and patterns of oceanic nutrient limitation, Nat. Geosci., 6, 701–710, https://doi.org/10.1038/NGEO1765, 2013.

Nelson, D. M. and Smith, W. O. J.: Sverdrup revisited: Critical depths, maximum chlorophyll levels and the control of Southern Ocean productivity by the irradiance-mixing regime, Limnol. Oceanogr., 36, 1650–1661, 1991.

Nicholson, S.-A., Lévy, M., Llort, J., Swart, S., and Monteiro, P. M. S.: Investigation into the impact of storms on sustaining summer primary productivity in the Sub-Antarctic Ocean, Geophys. Res. Lett., 43, 9192–9199, https://doi.org/10.1002/2016GL069973, 2016.

Nielsdóttir, M. C., Bibby, T. S., Moore, C. M., Hinz, D. J., Sanders, R., Whitehouse, M., Korb, R., and Achterberg, E. P.: Seasonal and spatial dynamics of iron availability in the Scotia Sea, Mar. Chem., 130, 62–72, https://doi.org/10.1038/345156a0, 2012.

Nowlin, W. D. and Klinck, J. M.: The physics of the Antarctic Circumpolar Current, Rev. Geophys., 24, 469–491, https://doi.org/10.1029/RG024i003p00469, 1986.

Obata, H., Karatani, H., and Nakayama, E.: Automated determination of iron in seawater by chelating resin concentration and chemiluminescence detection, Anal. Chem., 65, 1524–1528, https://doi.org/10.1021/ac00059a007, 1993.

Orsi, A. H., Whitworth III, T. W., and Nowlin, W. D.: On the meridional extent and front of the Antarctic Circumpolar Current, Deep.-Sea. Res. Pt. 1, 42, 641–673, https://doi.org/10.1016/0967-0637(95)00021-W, 1995.

Pakhomov, E. A. and Froneman, P. W.: Zooplankton dynamics in the eastern Atlantic sector of the Southern Ocean during austral summer 1997/1998, Deep.-Sea. Res. Pt. 1, 51, 2599–2616, https://doi.org/10.1016/j.dsr2.2000.11.001, 2004.

Parkhill, J., Maillet, G., and Cullen, J. J.: Fluorescence-based maximal quantum yield for PSII as a diagnostic of nutrient stress, J. Phycol., 37, 517–529, https://doi.org/10.1046/j.1529-8817.2001.037004517.x, 2001.

Price, N. M.: The elemental stoichiometry and composition of an iron-limited diatom, Limnol. Oceanogr., 50, 1149–1158, 2005.

Price, N. M., Ahner, B. A., and Morel, F. M. M.: The equatorial Pacific Ocean: Grazer-controlled phytoplankton populations in an iron-limited ecosystem, Limnol. Oceanogr., 39, 520–534, https://doi.org/10.4319/lo.1994.39.3.0520, 1994.

Racault, M.-F., Le Quéré, C., Buitenhuis, E., Sathyendranath, S., and Platt, T.: Phytoplankton phenology in the global ocean, Ecol. Indic., 14, 152–163, https://doi.org/10.1016/j.ecolind.2011.07.010, 2012.

Ras, J., Claustre, H., and Uitz, J.: Spatial variability of phytoplankton pigment distributions in the Subtropical South Pacific Ocean: comparison between in situ and predicted data, Biogeosciences, 5, 353–369, https://doi.org/10.5194/bg-5-353-2008, 2008.

Raven, J. A.: Predictions of Mn and Fe use efficiencies of phototrophic growth as a function of light availability for growth and C assimilation pathway, New. Phytol., 116, 1–18, https://doi.org/10.1111/j.1469-8137.1990.tb00505.x, 1990.

Raven, J. A., Evans, M. C., and Korb, R. E.: The role of trace metals in photosynthetic electron transport in O_2-evolving organisms, Photosynth. Res., 60, 111–150, https://doi.org/10.1023/A:1006282714942, 1999.

Rio, M. H., Guinehut, S., and Larnicol, G.: New CNES-CLS09 global mean dynamic topography computed from the combination of GRACE data, altimetry, and in situ measurements, J. Geophys. Res., 116, C07018, https://doi.org/10.1029/2010JC006505, 2011.

Roháček, K.: Chlorophyll Fluorescence Parameters: The Definitions, Photosynthetic Meaning, and Mutual Relationships, Photosynthetica, 40, 13–29, https://doi.org/10.1023/A:1020125719386, 2002.

Ryan-Keogh, T. J., Macey, A. I., Cockshutt, A. M., Moore, C. M., and Bibby, T. S.: The cyanobacterial chlorophyll-binding-protein IsiA acts to increase the in vivo effective absorption cross-section of photosystem I under iron limitation, J. Phycol., 48, 145–154, https://doi.org/10.1111/j.1529-8817.2011.01092.x, 2012.

Ryan-Keogh, T. J., Macey, A. I., Nielsdóttir, M., Lucas, M. I., Steigenberger, S. S., Stinchcombe, M. C., Achterberg, E. P., Bibby, T. S., and Moore, C. M.: Spatial and temporal development of phytoplankton iron stress in relation to bloom dynamics in the high-latitude North Atlantic Ocean, Limnol. Oceanogr., 58, 533–545, https://doi.org/10.4319/lo.2013.58.2.0533, 2013.

Ryan-Keogh, T. J., DeLizo, L. M., Smith Jr., W. O., Sedwick, P. N., McGillicuddy Jr., D. J., Moore, C. M., and Bibby, T. S.: Temporal progression of photosynthetic strategy by phytoplankton in the Ross Sea, Antarctica, J. Marine Syst., 166, 87–96, https://doi.org/10.1016/j.jmarsys.2016.08.014, 2017a.

Ryan-Keogh, T. J., Thomalla, S. J., Mtshali, T. N., and Little, H.: Modelled estimates of spatial variability of iron stress in the Atlantic sector of the Southern Ocean, Biogeosciences, 14, 3883–3897, https://doi.org/10.5194/bg-14-3883-2017, 2017b.

Sarthou, G., Baker, A. R., Blain, S., Achterberg, E. P., Boye, M., Bowie, A. R., Croot, P., Laan, P., de Baar, H. J. W., Jickells, T. D., and Worsfold, P. J.: Atmospheric iron deposition and sea-surface dissolved iron concentrations in the eastern Atlantic Ocean, Deep-Sea Res. Pt. I, 50, 1339–1352, https://doi.org/10.1016/S0967-0637(03)00126-2, 2003.

Schlitzer, R.: Carbon export fluxes in the Southern Ocean: results from inverse modeling and comparion with satellite-based estimates, Deep.-Sea. Res. Pt. 1, 49, 1623–1644, https://doi.org/10.4319/lo.1994.39.3.0520, 2002.

Schrader, P. S., Milligan, A. J., and Behrenfeld, M. J.: Surplus Photosynthetic Antenna Complexes Underlie Diagnostics of Iron Limitation in a Cyanobacterium, PLoS ONE, 6, e18753, https://doi.org/10.1371/journal.pone.0018753, 2011.

Shi, T., Sun, Y., and Falkowski, P. G.: Effects of iron limitation on the expression of metabolic genes in the marine cyanobacterium Trichodesmium erythraeum IMS101, Environ. Microbiol., 9, 2945–2956, https://doi.org/10.1111/j.1462-2920.2007.01406.x, 2007.

Siegel, D. A., Doney, S. C., and Yoder, J. A.: The North Atlantic spring phytoplankton bloom and Sverdrup's critical depth hypothesis, Science, 296, 730–733, https://doi.org/10.1126/science.1069174, 2002.

Smetacek, V., Assmy, P., and Henjes, J.: The role of grazing in structuring Southern Ocean pelagic ecosystems and biogeochemical cycles, Antarct. Sci., 16, 541–558, https://doi.org/10.1017/S0954102004002317, 2004.

Stramski, D., Reynolds, R. A., Kahru, M., and Mitchell, B. G.: Estimation of Particulate Organic Carbon in the Ocean from Satellite Remote Sensing, Science, 285, 239–242, https://doi.org/10.1126/science.285.5425.239, 1999.

Strzepek, R. F. and Harrison, P. J.: Photosynthetic architecture differs in coastal and oceanic diatoms, Nature, 431, 689–692, https://doi.org/10.1038/nature02954, 2004.

Strzepek, R. F., Hunter, K. A., Frew, R. D., Harrison, P. J., and Boyd, P. W.: Iron-light interactions differ in Southern Ocean phytoplankton, Limnol. Oceanogr., 57, 1182–1200, https://doi.org/10.4319/lo.2012.57.4.1182, 2012.

Strzepek, R. F., Maldonado, M. T., Hunter, K. A., Frew, R. D., and Boyd, P. W.: Adaptive strategies by Southern Ocean phytoplankton to lessen iron limitation: Uptake of organically complexed iron and reduced cellular iron requirements, Limnol. Oceanogr., 56, 1983–2002, https://doi.org/10.4319/lo.2011.56.6.1983, 2011.

Suggett, D. J., Moore, C. M., Hickman, A. E., and Geider, R. J.: Interpretation of fast repetition rate (FRR) fluorescence: signatures of phytoplankton community structure versus physiological state, Mar. Ecol. Prog. Ser., 376, 1–19, https://doi.org/10.3354/meps07830, 2009.

Sunda, W. G. and Huntsman, S. A.: Interrelated influence of iron, light and cell size on marine phytoplankton growth, Nature, 390, 389–392, https://doi.org/10.1038/37093, 1997.

Sverdrup, H. U.: On conditions for the vernal blooming of phytoplankton, Journal du Conseil International pour l'Exploration de la Mer, 18, 287–295, 1953.

Swart, S., Speich, S., Ansorge, I. J., and Lutjeharms, J. R. E.: An altimetry-based gravest empirical mode south of Africa: 1. Development and validation, J. Geophys. Res., 115, C03002, https://doi.org/10.1029/2009JC005299, 2010.

Swart, S., Chang, N., Fauchereau, N., Joubert, W. R., Lucas, M., Mtshali, T., Roychoudhury, A., Tagliabue, A., Thomalla, S., Waldron, H. N., and Monteiro, P. M. S.: Southern Ocean Seasonal Cycle Experiment 2012: Seasonal scale climate and carbon cycle links, S. Afr. J. Sci., 108, 11–13, https://doi.org/10.4102/sajs.v108i3/4.1089, 2012.

Swart, S., Thomalla, S. J., and Monteiro, P. M. S.: The seasonal cycle of mixed layer dynamics and phytoplankton biomass in the Sub-Antarctic Zone: A high-resolution glider experiment, J. Marine Syst., 147, 103–115, https://doi.org/10.1016/j.jmarsys.2014.06.002, 2015.

Tagliabue, A., Sallée, J.-B., Bowie, A. R., Lévy, M., Swart, S., and Boyd, P. W.: Surface-water iron supplies in the Southern Ocean sustained by deep winter mixing, Nat. Geosci., 7, 314–320, https://doi.org/10.1038/ngeo2101, 2014.

Thomalla, S. J., Fauchereau, N., Swart, S., and Monteiro, P. M. S.: Regional scale characteristics of the seasonal cycle of chlorophyll in the Southern Ocean, Biogeosciences, 8, 2849–2866, https://doi.org/10.5194/bg-8-2849-2011, 2011

Thomalla, S. J., Racault, M.-F., Swart, S., and Monteiro, P. M. S.: High-resolution view of the spring bloom initiation and net community production in the Subantarctic Southern Ocean using glider data, ICES, J. Mar. Sci., 72, 1999–2020, https://doi.org/10.1093/icesjms/fsv105, 2015.

Thomalla, S. J., Moutier, W., Ryan-Keogh, T. J., Gregor, L., and Schütt, J.: An optimized method for correcting fluorescence quenching using optical backscattering on autonomous platforms, Limnol. Oceanogr.-Meth., 16, 132–144, https://doi.org/10.1002/lom3.10324, 2017.

Welschmeyer, N. A.: Fluorometric analysis of chlorophyll-a in the presence of chlorophyll-b and pheopigments, Limnol. Oceanogr., 39, 1985–1992, https://doi.org/10.4319/lo.1994.39.8.1985, 1994.

Westberry, T., Behrenfeld, M. J., Siegel, D. A., and Boss, E.: Carbon-based primary productivity modeling with vertically resolved photoacclimation, Global Biogeochem. Cy., 22, GB2024, https://doi.org/10.1029/2007GB003078, 2008.

Westberry, T. K., Schultz, P., Behrenfeld, M. J., Dunne, J. P., Hiscock, M. R., Maritorena, S., Sarmiento, J. L., and Siegel, D. A.: Annual cycles of phytoplankton biomass in the subarctic Atlantic and Pacific Ocean, Global Biogeochem. Cy., 30, 175–190, https://doi.org/10.1002/2015GB005276, 2016.

Wolters, M.: Quickchem Method 31-114-27-1-D – Silicate in Brackish or Seawater, Lachat Instruments, Colorado, USA, 2002.